

Stress-mediated reprogramming of prostate cancer one-carbon cycle drives disease progression

Pällmann, Nora¹; Deng, Ke²; Livgård, Marte^{1,2}; Tesikova, Martina³; Jin, Yixin¹; Frengen, Nicolai Sebastian¹; Kahraman, Nermin⁴; Mokhlis, Hamada M.^{4,5}; Ozpolat, Bulent⁴; Kildal, Wanja²; Danielsen, Håvard Emil^{2,6,7,8}; Fazli, Ladan⁹; Rennie, Paul S.⁹; Banerjee, Partha P.¹⁰; Üren, Aykut¹¹; Jin, Yang¹; Kuzu, Omer F.¹; Saatcioglu, Fahri^{1,2}

¹Department of Biosciences, University of Oslo, Norway;

²Institute for Cancer Genetics and Informatics, Oslo University Hospital, Norway;

³Department of Mathematics and Science, University of South-Eastern Norway;

⁴Gynecological Oncology, MD Anderson Cancer Center, Houston, TX, USA;

⁵Department of Pharmacology and Toxicology, Faculty of Pharmacy, Al-Azhar University, Cairo, Egypt;

⁶Center for Cancer Biomedicine, University of Oslo, Norway;

⁷Department of Informatics, University of Oslo, Norway;

⁸Nuffield Division of Clinical Laboratory Sciences, University of Oxford, UK;

⁹The Vancouver Prostate Centre, Vancouver, BC, Canada;

¹⁰Department of Biochemistry, Molecular and Cellular Biology, Georgetown University Medical Center, Washington, DC, USA;

¹¹Lombardi Comprehensive Cancer Center, Georgetown University, Washington, DC, USA.

This article has been accepted for publication and undergone full peer review but has not been through the copyediting, typesetting, pagination, and proofreading process, which may lead to differences between this version and the Version of Record.

Pällmann, N., Deng, K., Livgård, M., Tesikova, M., Jin, Y., Frengen, N. S., Kahraman, N., Mokhlis, H. M., Ozpolat, B., Kildal, W., Danielsen, H. E., Fazli, L., Rennie, P. S., Banerjee, P. P., Üren, A., Jin, Y., Kuzu, O. F. & Saatcioglu, F. (2021). Stress-Mediated Reprogramming of Prostate Cancer One-Carbon Cycle Drives Disease Progression. *Cancer Research*, 81(15), 4066-4078.
<https://doi.org/10.1158/0008-5472.CAN-20-3956>

30 **Abstract**

31 One carbon (1C) metabolism has a key role in metabolic programming with both
32 mitochondrial (m1C) and cytoplasmic (c1C) components. Here we show that
33 Activating Transcription Factor 4 (ATF4) exclusively activates gene expression
34 involved in m1C, but not c1C cycle in prostate cancer (PCa) cells. This includes
35 activation of Methylenetetrahydrofolate dehydrogenase 2(MTHFD2) expression, the
36 central player in the m1C cycle. Consistent with the key role of m1C cycle in PCa,
37 MTHFD2 knockdown inhibited PCa cell growth, prostatosphere formation and growth
38 of patient-derived xenograft (PDX) organoids. In addition, therapeutic silencing of
39 MTHFD2 by systemically administered nanoliposomal siRNA profoundly inhibited
40 tumor growth in a preclinical PCa mouse model. Consistently, MTHFD2 expression is
41 significantly increased in human PCa and a gene expression signature based on the
42 m1C cycle has significant prognostic value. Furthermore, MTHFD2 expression is
43 coordinately regulated by ATF4 and the oncoprotein c-MYC, which has been
44 implicated in PCa. These data suggest that the m1C cycle is essential for PCa
45 progression and may serve as a novel biomarker and therapeutic target.

46 **Significance**

47 Here, we demonstrate that the mitochondrial, but not cytoplasmic, one-carbon cycle
48 has a key role in prostate cancer cell growth and survival and may serve as a
49 biomarker and/or therapeutic target.

50 **Introduction**

51 Cell proliferation requires energy, the availability of building blocks for new cellular
52 components, and the ability to maintain cellular redox homeostasis (1). For building
53 block generation and redox homeostasis, amino acid metabolism involving serine and
54 glycine, and the carbon units that they provide, are essential (2). The 1C cycle
55 mediates the folate-mediated transfer of 1C units from donor molecules, mainly
56 serine, to acceptor molecules, such as purines, methionine and thymidylate; this is
57 necessary for essential cellular processes including DNA synthesis, DNA repair, and
58 the maintenance of cellular redox status.

59 Eukaryotic cells have complementary pathways for 1C metabolism in the cytosol and
60 mitochondria comprising distinct serine hydroxymethyltransferases (SHMTs) and
61 methylenetetrahydrofolate dehydrogenases (MTHFDs). While the cytoplasmic 1C
62 pathway (c1C) prevails in non-proliferating somatic tissues, the mitochondrial
63 pathway (m1C) is predominantly active in proliferating cells, as well as in cancer cells
64 (3). In fact, the central player of the m1C cycle, methylenetetrahydrofolate
65 dehydrogenase 2 (MTHFD2), is overexpressed in many different tumor types (4).
66 MTHFD2 is also critical during embryonic development (5), but is typically not
67 expressed in normal adult tissues, except in highly proliferative cells, such as during
68 T-cell lymphocyte activation (4,6).

69 While MTHFD2 is implicated in various cancers, little is known about its potential role
70 in prostate cancer (PCa), which is the most frequently diagnosed noncutaneous
71 cancer and the second most common cause of cancer death in men (7). The
72 androgen receptor (AR) plays a key role in normal prostate growth, as well as in
73 prostate carcinogenesis and progression. We previously found that AR signaling, a
74 central driver of PCa, increased expression of activating transcription factor 4 (ATF4)
75 (8). We have recently found that ATF4 has essential pro-survival functions in PCa
76 cells *in vitro* and *in vivo* through direct activation of a broad range of genes including
77 key metabolic pathways (9).

78 Here, we show that ATF4 directly and specifically regulates expression of genes
79 encoding m1C cycle enzymes in PCa cells. Among these, MTHFD2 is critical for
80 PCa growth *in vitro* and *in vivo*, and may serve as a novel therapeutic target. In
81 addition, the oncoprotein c-MYC interplays with ATF4 in regulating MTHFD2
82 expression establishing a new mode of action for c-MYC in PCa.

83 **Materials and Methods**

84 **Cell culture**

85 293T, RWPE1, LNCaP, DU145, and 22Rv1 cell lines were purchased from the
86 American Type Culture Collection (Rockville, MD). The VCaP, C4-2B, and LNCaP-c-
87 MYC cell lines were kind gifts from Dr. Frank Smit (Radboud University Nijmegen
88 Medical Centre, The Netherlands), Dr. Lelund Chung (Cedars-Sinai Medical Center,
89 CA), and Dr. Ian G. Mills (Oslo University Hospital, Norway), respectively. Cells were
90 routinely maintained in a humidified 5% CO₂ and 95% air incubator at 37°C. PCa
91 cells were cultured in RPMI 1640, and 293T cells in DMEM, containing 10% fetal calf
92 serum, 50 U/ml penicillin, 50 µg/ml streptomycin, and 4 mM L-glutamine (all
93 purchased from BioWhittaker-Cambrex). Where indicated, cells were treated with 30
94 nM Thapsigargin (Tg) (Sigma-Aldrich) for 5 h, unless stated otherwise. All cell lines
95 were used within 15 passages after reviving from the frozen stocks and routinely
96 tested and were free of mycoplasma contamination.

97

98 **Ectopic expression of ATF4**

99 ATF4 ORF entry clone was obtained from the Arizona State University plasmid
100 repository (HsCD00073682) and cloned into doxycycline-inducible pLIX_403
101 destination vector (Addgene #41395), a gift from Dr. David Root, through standard
102 gateway cloning procedure. Viruses were produced by transfecting HEK293T cells
103 with packaging (psPAX2), envelope (pMD2.G), and pLIX403-ATF4 plasmids, using
104 Lipofectamine 3000 reagent. LNCaP cells were then transduced with the harvested
105 lentivirus.

106 **Cell proliferation and viability assays**

107 Briefly, cells were reverse transfected using Lipofectamine RNAiMAX transfection
108 reagent (ThermoFisher) and plated into 96-well or 6-well plates. Cells in 6-well plates
109 were cultured for the indicated times, trypsinized, stained with trypan blue, and
110 counted using a hemocytometer. The data shown are representative of at least three
111 independent experiments performed in triplicate. Cells plated into the 96-well plates
112 were cultured for 48 hrs and cell viability was measured using the CCK-8 kit (Bimake,
113 Munich, Germany).

114 **Colony formation and prostatosphere assays**

115 Cells were trypsinized, seeded at a density of 5,000 cells per well into 6-well plates,
116 and cultured for 2-3 weeks. The cells were then fixed with methanol and stained with
117 0.4% crystal violet. Colonies were quantified by extracting crystal violet in 10% acetic
118 acid and measurement of absorbance at 590 nm. Prostatosphere assays were
119 performed as described previously (10). The data shown are representative of at
120 least two independent experiments performed in triplicate.

121 **Quantitative PCR**

122 RNA extraction, reverse transcription and quantitative polymerase chain reaction
123 (qPCR) were performed as described previously (8). The values were normalized to
124 the relative amount of the internal standard *GAPDH*, *TBP*, or *ACTB*. Results
125 normalized to *GAPDH* are presented unless indicated otherwise. PCR primer
126 sequences are available upon request. The data shown are representative of at least
127 two independent experiments performed in triplicate.

128 **Western analysis**

129 Whole-cell extracts and Western analyses were performed by standard methods as
130 described previously (8). The antibodies used were: ATF4 (11815, Cell Signaling),
131 ATF4 (A5514, Bimake), ASNS (146811AP) (Proteintech); MTHFD2 (sc-390708),
132 GAPDH (sc-47274), β -Actin (sc-47778) (Santa Cruz Biotechnology). All antibodies
133 were used at a dilution of 1:1,000, except for MTHFD2 (1:100), GAPDH (1:5,000) and
134 β -Actin (1:2,000). The data shown are representative of at least two independent
135 experiments.

136 **Other methods**

137 Descriptions of the cell culture, RNA interference, chromatin immunoprecipitation
138 (ChIP), ChIP-Seq, patient-derived xenograft organoids, mitochondrial membrane
139 potential assay, nanoliposomal siRNA targeting in PCa xenografts,
140 immunohistochemistry (IHC), and bioinformatics analysis are available as
141 Supplementary Materials.

142 **Statistical analysis**

143 Mean and standard deviation values were calculated using Microsoft Excel software.
144 The potential effects were evaluated using Student's two-sided t-test unless indicated
145 otherwise. Values of $p < 0.05$ were considered as significant. Statistically significant
146 differences are denoted by *, **, and *** indicating $p < 0.05$, $p < 0.01$ and $p < 0.001$,
147 respectively. Error bars indicate SEM.

148 **Results**

149 **ATF4 specifically activates the mitochondrial one-carbon cycle in PCa**

150 To decipher novel ATF4 targets that may play essential roles in PCa, we performed a
151 ChIP-Seq experiment and identified ATF4 binding sites in LNCaP cells upon Tg
152 treatment. This analysis revealed 7488 ATF4 binding sites in close proximity (± 1000
153 bp) to the transcription start sites of 5597 protein-coding genes (**Supp. Table 1**).
154 There was a significant overlap between these binding sites with those that were
155 previously identified in various tissues or cell lines in the Gene Transcription
156 Regulation Database (GTRD), suggesting effective capture of target sequences
157 (**Supp. Figure 1A, Supp. Table 2**). To assess the potential functionality of
158 the binding sites, we analyzed these data together with our data from global
159 transcriptomic and proteomic analyses upon siRNA-mediated ATF4 knockdown in
160 Tg-treated LNCaP cells (9). Among the genes identified by ChIP-Seq, 29 were
161 downregulated in both transcriptomic and proteomic analyses (**Figure 1A, Supp.**
162 **Table 3**). In addition to well-established ATF4 target genes, such as Asparagine
163 Synthetase (ASNS) and Phosphoserine Phosphatase (PSPH), two 1C metabolism
164 genes, MTHFD2 and MTHFD1L were among these 29 genes. Another 1C

165 metabolism gene, SHMT2, also harbored an ATF4 binding site and was among the
166 downregulated genes in the microarray experiment (**Figure 1A**). Intriguingly,
167 although mammalian 1C metabolism is comprised of two parallel pathways (cytosolic
168 and mitochondrial) with almost identical core enzymatic capabilities (11), all three
169 identified ATF4-regulated 1C metabolism genes belong to the mitochondrial pathway
170 (**Figures 1B**). Notably, the identified ATF4 binding sites in the vicinity of m1C cycle
171 genes overlapped with ATF4 binding sites that have been reported in the Gene
172 Transcription Regulation Database, and were highly conserved among various
173 mammalian genomes (**Figure 1C**). In contrast, expression of two c1C metabolism
174 genes (SHMT1 or MTHFD1) was not affected; consistently, they did not harbor any
175 ATF4 binding sites near their TSS (**Supp. Figure 1B**). Consistent with this
176 observation, in the great majority of the 16 distinct cancer types, *ATF4* or and its
177 target *ASNS* mRNA levels were highly correlated with m1C, but not c1C, enzyme
178 gene expression (**Supp. Figure 1C**). Moreover, analyses of the protein and mRNA
179 expression data from the Cancer Cell Line Encyclopedia dataset showed significant
180 correlations between ATF4 protein levels and expression of the m1C, but not c1C
181 enzymes (**Supp. Figure 2**). In fact, in this dataset, after Sperm flagellar protein 2
182 (SPEF2) (its functional role in PCa, if any, is currently not known), *MTHFD2* is the
183 second gene with the highest correlation to protein levels of ATF4. Similarly, there
184 was a high correlation between *ASNS* and m1C cycle enzyme gene expression.
185 Evaluation of 1C metabolism gene expression in the Oncomine database revealed
186 that m1C pathway genes are more consistently upregulated in diverse cancers
187 compared to c1C genes (**Figure 1D**). Additionally, CRISPR-based cancer cell line
188 dependency profiles of the 1C metabolism genes showed a significant correlation
189 between the mitochondrial, but not cytosolic, members of the pathway (**Figure 1E**).
190 These data suggested that ATF4 is involved in mediating m1C metabolism gene
191 expression in PCa.

192 We next examined 1C metabolism gene expression upon siRNA mediated
193 knockdown of *ATF4* in three independent PCa cell lines. *ATF4*-specific siRNAs
194 effectively hindered expression of well-known ATF4 target genes such as
195 Phosphoglycerate Dehydrogenase (*PHGDH*), Phosphoserine Aminotransferase 1

196 (*PSAT1*) and *PSPH* in the LNCaP, VCaP, and 22Rv1 cell lines (**Figure 2A, and**
197 **Supp. Figures 3A-B**), while Tg-mediated stimulation of ATF4 expression increased
198 their expression (**Figure 2B**). Consistent with the ChIP-Seq experiment, m1C gene
199 expression for *SHMT2*, *MTHFD2*, and *MTHFD1L* were decreased upon *ATF4*
200 silencing and increased upon Tg-mediated ATF4 activation (**Figure. 2A-B, and**
201 **Supp. Figures 3A-B**). In contrast, neither *ATF4* silencing nor *ATF4* induction
202 significantly affected expression of c1C cycle genes *SHMT1* and *MTHFD1* (**Figures.**
203 **2A-B, Supp. Figures 3A-B**). Moreover, in a previously published RNA-Seq dataset
204 (12), treatment of LNCaP cells with Tunicamycin (Tm - an inducer of ER stress/ATF4
205 pathway through inhibition of N-linked glycosylation in the endoplasmic reticulum)
206 also resulted in the expression of m1C genes in an ATF4 dependent manner (**Figure**
207 **2C**). We validated the Tm-induced upregulation of m1C genes in LNCaP and PC3
208 cell lines (**Supp. Figures 3C-D**). In Tg-treated cells, ATF4 knockdown effectively
209 reduces MTHFD2 protein levels (**Figure 2D**), and ectopic expression of ATF4
210 effectively rescues it back to control levels (**Figure 2E**). In contrast, in non-stressed
211 LNCaP cells, knockdown of ATF4 does not alter MTHFD2 mRNA or protein levels, as
212 under these conditions, despite significant mRNA levels, ATF4 is not translated into
213 protein (**Figure 2F, bottom panel**). However, ectopic ATF4 expression effectively
214 increased both mRNA and protein levels of MTHFD2. Interestingly, without
215 knockdown of endogenous ATF4 expression, ectopically introduced *ATF4* mRNA was
216 not detectable (**Figure 2F, upper panel**). This was due to the downregulation of
217 endogenous ATF4 mRNA expression upon induction of ectopic ATF4 and suggested
218 an autoregulatory negative feedback loop by ATF4 on its transcription. Consistent
219 with these findings, ATF4 binding to the vicinity of the *MTHFD2* gene was verified by
220 ChIP and *ATF4* silencing abolished this interaction (**Figure 2G**). Taken together,
221 these data establish ATF4 as a key regulator of the m1C, but not the c1C, cycle gene
222 expression.

223 **MTHFD2 is critical for PCa cell growth *in vitro* and *in vivo***

224 Since MTHFD2 has a key role in the m1C cycle (13) and was previously implicated in
225 cancer (4), we assessed whether it affects PCa cell growth. siRNA-mediated

226 *MTHFD2* silencing effectively reduced its mRNA and protein levels (**Figure 3A**).
227 *MTHFD2* knockdown was maximal (~80%) at 72 hours post-transfection and
228 remained significantly downregulated for more than one week, but returned back to
229 basal levels by day 12 (**Supp. Figure 4A**). Short term *MTHFD2* knockdown
230 significantly reduced the viability (**Supp. Figure 4B**) and long-term knockdown nearly
231 abolished both viability and colony formation ability of LNCaP, DU145, VCaP, and
232 22Rv1 cells (**Figures 3B-D**). Furthermore, *MTHFD2* knockdown significantly
233 hindered LNCaP and DU145 prostatosphere growth (**Figure 3E**). However, viability
234 of a normal prostate epithelial cell line, RWPE1, was not affected by *MTHFD2*
235 knockdown (**Figure 3F**).

236 To further evaluate the potential effects of *MTHFD2* on PCa growth, organoids of
237 LuCaP patient-derived xenograft (PDX) models were used (14). Three of the six
238 analyzed LuCaP organoids expressed high levels of *MTHFD2* expression (**Figure**
239 **3G**). Three organoids, two with high expression and one with low expression, were
240 analyzed further. These three PDX models, LuCaP 35, LuCaP 96, and LuCaP 136,
241 express AR, lack PTEN expression, and were developed from lymph node
242 metastasis, localized PCa, and adenocarcinoma cells from ascites, respectively (14).
243 siRNA-mediated *MTHFD2* knockdown effectively suppressed formation of LuCaP35
244 and LuCaP96 organoids that express high levels of *MTHFD2* without inducing cell
245 death (**Figure 3G-H**; quantification is presented in **Supp. Figure 4C**). On the other
246 hand, LuCaP 136 organoid that expresses very low levels of *MTHFD2* was not affe
247 cted by *MTHFD2* knockdown.

248 To assess the therapeutic potential of *MTHFD2* inhibition *in vivo*, we performed
249 xenograft experiments as previously described(15,16). VCaP or 22Rv1 cells were
250 subcutaneously injected into male nude mice. Upon formation of palpable tumors,
251 empty nanoliposomes or those that carry *MTHFD2*-specific siRNA were administered
252 by intraperitoneal injection and tumor growth was monitored over time. Whereas
253 tumors continued to grow rapidly in mice injected with the empty nanoliposomes,
254 injection of nanoliposomes containing *MTHFD2*-specific siRNA dramatically inhibited
255 tumor growth in both models (**Figure 3I**). Nanoliposomal si*MTHFD2* delivery was

256 well-tolerated and did not result in any weight loss (**Supp. Figure 4D**) Together with
257 the findings from above, these data suggest that MTHFD2 is critical for PCa growth
258 and may serve as a novel therapeutic target.

259 **MTHFD2 expression is up-regulated in human PCa specimens**

260 Both mRNA and protein expression of MTHFD2 were robust in the normal prostate
261 cell line RWPE1 and in all of the PCa cell lines tested, with some variability in the
262 level of expression (**Figure 4A**). We next evaluated MTHFD2 expression in 24
263 human PCa specimens and their corresponding benign tissues from the same
264 patients using immunohistochemistry. MTHFD2 expression was significantly
265 increased in PCa compared to benign specimens (**Figure 4B**). This observation was
266 verified by an independent tissue microarray cohort consisting of 860 PCa and 223
267 benign prostate specimens (**Figure 4C**). In this large cohort, MTHFD2 expression
268 also correlated with the Gleason score indicating that it may have prognostic value.
269 Importantly, ATF4 and MTHFD2 protein expression was correlated in a sample
270 subset of this TMA (**Figure 4D**). These data show that MTHFD2 expression is
271 significantly increased in PCa compared with normal tissue.

272 **m1C gene expression signature is strongly associated with PCa** 273 **prognosis**

274 To assess whether ATF4-regulated m1C cycle gene expression could serve as a
275 potential prognostic biomarker for PCa, we analyzed MTHFD2, SHMT2, MTHFD1L,
276 and MTHFD2L expression in five independent PCa cohorts in the Oncomine
277 database (17-21). MTHFD2 expression was consistently and significantly
278 upregulated in primary and metastatic PCa compared to benign samples (**Figure 5A**).
279 SHMT2 was upregulated in three of the five cohorts (**Figure 5B**). Only three cohorts
280 had expression data for MTHFD1L and two for MTHFD2L. MTHFD1L was
281 significantly upregulated in the primary and metastatic tumors while MTHFD2L was
282 upregulated in one of the two cohorts (**Supp. Figure 5**). In addition, in the Cancer
283 Genome Atlas dataset, m1C metabolism gene expression, but not the cytosolic
284 counterparts, were more prominently upregulated in primary tumor samples (**Figure**
285 **5C**). These data led us to evaluate whether m1C metabolism gene expression may

286 have prognostic value. Indeed, a gene expression signature consisting of the three
287 m1C cycle enzymes (MTHFD2, MTHFD1L, and SHMT2) was significantly associated
288 with recurrence-free survival in PCa patients (**Figure 5D**). Taken together, these
289 observations suggest that activation of ATF4-regulated m1C metabolism could serve
290 as a prognostic biomarker in PCa.

291 **mTOR/ATF4 signaling regulates m1C expression in normal prostate but** 292 **not in PCa**

293 Previous work has shown that mTORC1 and PERK/eIF2A signaling regulate cell
294 metabolism by controlling ATF4 levels (22,23). To assess the impact of mTORC1
295 signaling on m1C metabolism in PCa, we investigated whether there is a correlation
296 between the expression of three ATF4-regulated m1C metabolism genes and those
297 that are specifically regulated by the mTORC1 signaling cascade. Genome-wide
298 transcriptional alterations were previously determined upon treatment of wild type or
299 ATF4 knockout human embryonic kidney (HEK) cells with Torin 1, a potent ATP-
300 competitive inhibitor of mTOR (22). We used these data to identify genes that are
301 exclusively regulated by mTORC1 signaling without input from the PERK/eIF2 α /ATF4
302 cascade. Sixty genes were significantly deregulated by more than ± 1.7 -fold upon
303 Torin 1 treatment in both cell lines. Since some of these genes could still be
304 regulated and influenced by ATF4, whose expression is in fact also low in normal
305 cells, we further narrowed this list by filtering out known or potential ATF4 target
306 genes that were compiled from various public databases resulting in 38 genes as
307 ATF4 independent targets of mTOR signaling (**Figure 6A**).

308
309 In the GTEX database, representing normal prostate samples, expression of majority
310 of the 38 genes were well correlated with m1C gene expression in the expected
311 direction (e.g. the genes inhibited by Torin 1 positively correlated with the investigated
312 genes) (**Figure 6A**). However, such a correlation was absent in the TCGA dataset,
313 representing primary PCa. Consistently, there was a significant overlap between the
314 top 500 genes that correlated with MTHFD2 expression in the SEEK database that
315 contains 78 microarray-based PCa gene expression datasets, and the TCGA PCa

316 dataset (188 genes, **Figure 6B**). However, only 62 genes were shared between
317 GTEX and SEEK, GTEX and TCGA, or in all three datasets. These 62 genes were
318 not enriched for any specific signaling pathway, but contained genes for several
319 translation factors (EEF1B2, EIF2S2, EIF3J, EIF4EBP1), genes that encode proteins
320 involved in RNA transport (STRAP, THOC7, RAN), and the gene encoding
321 mitochondrial folate transporter SLC25A32 (**Supp. Table 4**). These results indicated
322 that m1C metabolism is distinctly regulated between normal prostate and PCa. In the
323 normal prostate, m1C metabolism appears to be primarily regulated by mTORC1
324 signaling, but in PCa another signaling pathway(s) may override this regulation.
325 Indeed, in LNCaP cells Tg-mediated induction of ER stress effectively supersedes
326 mTORC1-mediated MTHFD2 regulation; in contrast to basal conditions, mTORC1
327 inhibitor rapamycin failed to downregulate ATF4-regulated m1C metabolism gene
328 expression upon Tg treatment (**Figure 6C**). These data suggest that m1C
329 metabolism is differentially regulated in PCa compared to normal prostate.

330 **c-MYC is a key mediator of m1C gene expression**

331 To assess which additional pathways could be involved in the regulation of m1C
332 metabolism, we performed gene set enrichment analysis on the top 500 genes that
333 correlate (Pearson $r > 0.4$) with the m1C gene expression signature in the TCGA
334 dataset (**Supp. Table 5**). As expected, genes involved in aminoacyl-tRNA
335 biosynthesis, 1C metabolism, cell cycle, and mitotic nuclear division were enriched
336 among the correlated genes (**Figure 6D**). In addition, according to both ENCODE
337 and ChEA databases, genes that are associated with c-MYC were exceptionally
338 highly enriched ($p = 8.96e^{-90}$ in ENCODE, $8.6e^{-44}$ in ChEA). Indeed, c-MYC
339 expression itself significantly correlated with the m1C gene signature ($r = 0.43$).
340 Moreover, the 188 genes that correlated well with MTHFD2 in both SEEK and TCGA
341 databases (**Figure 6B**) were also highly enriched for c-MYC-mediated regulation
342 ($p = 1.15e^{-50}$ in Encode, $p = 1.18e^{-17}$ in ChEA) (**Supp. Table 4**). These results
343 suggested that c-MYC may be involved in mediating the effects of m1C gene
344 expression in PCa.

345

346 We next determined whether m1C gene expression signature may be associated with
347 mutational events in PCa. Comparison of the mutation prevalence between the top
348 and bottom 180 samples based on the expression of the m1C gene expression
349 signature in the TCGA dataset revealed several enriched copy number alterations
350 and point mutations (**Figure 6E**). Increased representation of 8p11 and 8p21-22
351 deletions, and c-MYC amplification among the signature-high group indicated that c-
352 MYC is involved in the regulation of m1C gene expression (**Figure 6E**) (24). 8p11
353 locus harbors the SFRP1 gene that encodes a Wnt signaling inhibitor that is
354 frequently inactivated in a variety of malignancies, including PCa, and has been
355 identified as an essential molecule in c-MYC-dependent transformation (25,26). In
356 the TCGA dataset, SFRP1 expression negatively correlated with those of *ATF4* ($r=-$
357 0.35), *ASNS* ($r = -0.33$) and m1C gene signature ($r= -0.28$) suggesting that loss of
358 SFRP1 could regulate m1C metabolism via ATF4 signaling. Similarly, loss of 8p21-
359 22 locus is one of the most frequent chromosomal aberrations in PCa and harbors
360 the *NKX3.1* gene that encodes a transcription factor, which acts as a tumor
361 suppressor by opposing c-MYC transcriptional activity (27). We further investigated
362 potential association of these mutations on m1C gene expression by assessing
363 expression of the three m1C genes in the mutated versus wild type samples in the
364 TCGA dataset (**Supp. Figure 6**). All three m1C cycle genes were significantly
365 upregulated in all of the eight investigated mutant subgroups. Taken together, these
366 data suggest that mutational events in PCa could activate m1C gene expression
367 through c-MYC.

368

369 We next examined m1C gene expression at the protein level using the recently
370 reported proteomics data from 375 cancer cell lines (28). Since the number of
371 mitochondria per cell would vary among different cancer cell lines and can skew the
372 results, we used the expression of mitochondrial encoded proteins MT-CO1 and MT-
373 ATP8 to filter out proteins that correlate with m1C metabolism gene expression
374 simply due to varying numbers of mitochondria in the different cell lines. There was a
375 significant overlap between the expression of proteins that correlated with MTHFD2
376 and SHMT2 expression, and these did not coincide with mitochondrial proteins

377 **(Figure 6F; Supp. Table 6)**. In contrast, although almost one-fourth of the proteins
378 that correlated with MTHFD1L expression were mitochondrial proteins, MTHFD1L did
379 not correlate well with MTHFD2 or SHMT2 protein expression; this suggests that in
380 contrast to MTHFD1L, MTHFD2 and SHMT2 expression is regulated independently
381 from mitochondrial biogenesis. Interestingly, mRNA processing, splicing, transport,
382 and mitochondrial translation-related proteins were highly enriched among the 136
383 proteins that were shared between the MTHFD2 and SHMT2 groups **(Figure 6F)**.
384 These proteins were also enriched for harboring a nearby c-MYC binding site in their
385 genes ($p = 1.23e^{-13}$) further indicating that c-MYC is a prominent player in the
386 regulation of m1C metabolism at the protein level **(Figure 6G)**.

387

388 **Under stress conditions, ATF4 counterbalances c-MYC loss to drive m1C gene**
389 **expression.**

390 A recent study has identified an intricate regulation of protein synthesis through c-
391 MYC-ATF4 cooperation, where c-MYC was involved in the regulation of EIF4EBP1
392 expression in an ATF4 dependent manner (29). We thus considered the possibility
393 that ATF4 and c-MYC may bind to adjacent or neighboring sites and coordinately
394 regulate m1C cycle gene expression. Intriguingly, data from ENCODE indicated that
395 all three ATF4-regulated m1C genes also harbor c-MYC binding sites that are in
396 close proximity, in fact almost overlapping, with the identified ATF4 binding sites
397 **(Supp. Figure 7)**. Moreover, the analysis of a previously published ChIP-Seq
398 experiment in LNCaP cells revealed c-MYC binding sites that overlap with those of
399 ATF4 that we have identified in the m1C genes and the EIF4EBP1 gene **(Figure 7A)**
400 (30). c-MYC binding to these sites was enriched upon its ectopic expression.
401 Furthermore, analysis of publicly available datasets revealed that m1C gene
402 expression was modulated upon ectopic expression or CRISPRi-mediated inhibition
403 of c-MYC **(Figures 7B-C)**. In these datasets, modulation of m1C gene expression
404 could not be attributed to an alteration upon cellular stress as in contrast to the report
405 by Tameria et al, indicators of ER stress (such as DDIT3, HERPUD1, ERLEC1,
406 PDIA4, PDIA6) were not deregulated by c-MYC induction or knockdown (29) **(Supp.**
407 **Figures 8A-B)**. We verified the effect of c-MYC on MTHFD2 expression in LNCaP

408 cells, where siRNA-mediated c-MYC knockdown resulted in a significant decrease in
409 MTHFD2 at both mRNA and protein levels (**Figure 7D**).

410

411 We next investigated whether ATF4 and c-MYC could synergistically regulate
412 MTHFD2 expression in PCa cells. To that end, we modulated the levels of the two
413 transcription factors by siRNA-mediated knockdown and assessed MTHFD2
414 expression, under basal and Tg-treated conditions. Under non-stressed conditions,
415 c-MYC knockdown effectively reduced mRNA and protein levels of MTHFD2, while
416 ATF4 knockdown had a slight effect (**Figure 7E**). In contrast, under Tg-induced
417 stress conditions, MTHFD2 expression was clearly dependent on ATF4 as Tg
418 induction, in a remarkable fashion, completely inhibited c-MYC expression, and ATF4
419 knockdown effectively decreased MTHFD2 levels (**Figure 7E**). These data suggest
420 that, along with ATF4, c-MYC is a key component of the regulatory network that
421 affects m1C gene expression.

422

423 **Discussion**

424 Metabolic reprogramming is critical for cancer cell growth and dissemination (31-33).
425 Some key determinants of this cellular rewiring have been established, but there is an
426 urgent need to identify the molecular mechanisms at play that can be targeted for
427 novel therapeutic approaches. We have recently found that ATF4 is critical for PCa
428 growth *in vitro* and *in vivo* (9). We now show that ATF4 makes significant
429 contributions to metabolic reprogramming of PCa cells by significantly increasing
430 m1C cycle gene expression (MTHFD2, MTHFD1L and SHMT2), without affecting
431 expression of their cytoplasmic counterparts (MTHFD1 and SHMT1). In particular,
432 we found that ATF4-driven deregulation of MTHFD2 expression promotes PCa cell
433 proliferation *in vitro* and *in vivo*. Consistently, a gene expression signature based on
434 the m1C cycle has significant prognostic value for PCa progression.

435 Previous studies have shown that ATF4 regulates metabolic pathways connected to
436 amino acid uptake, tRNA synthesis, and transport (34,35). In particular, ATF4 is a
437 major regulator of the serine biosynthesis pathway that is upregulated and is

438 associated with poor prognosis in various cancers (2,36-38). Conversion of serine
439 into glycine and formate is catalyzed by the m1C cycle enzymes in three metabolic
440 steps (**Figure 1B**); by concurrently regulating these two cascades, ATF4 enables *de*
441 *novo* synthesis of purines, thymidylate, and glutathione which are essential for rapidly
442 proliferating cells.

443 It is currently not known what could be the benefit for cancer cells to preferentially use
444 the m1C cycle, rather than the cytosolic counterpart. The products of the m1C cycle,
445 formate and glycine, are transported to the cytosol, where formate is metabolized
446 back to 10-Formyltetrahydrofolate (CHO–THF) to serve as a substrate for purine
447 synthesis (39). Although the c1C cycle could also drive purine synthesis by yielding
448 CHO–THF, the m1C pathway provides the dominant flux for purine synthesis (40).
449 However, neither formate nor glycine treatment was able to recover the viability of
450 PCa cells upon MTHFD2 knockdown (**Supp. Figure 9**) suggesting that m1C
451 metabolism plays other essential roles beyond supplying the building blocks for
452 nucleotide biosynthesis.

453 One possibility in this regard is the potential contribution of m1C cycle to the energy
454 and redox demands of proliferating cells by generation of ATP and NADH/NADPH
455 (3,41). In the m1C cycle, the reaction catalyzed by MTHFD2 is a significant source of
456 NADH, which can be used in oxidative phosphorylation to generate 2.5 ATPs, and the
457 reaction catalyzed by MTHFD1L itself generates an ATP molecule giving an overall
458 yield of 3.5 ATPs per cycle (3). Moreover, NADH production by the m1C cycle could
459 contribute to PCa development by enhancing the antioxidant defense of cancer cells
460 (42,43). Consistently, inhibition of MTHFD2 and SHMT2 expression has been
461 reported to disturb redox homeostasis and impair cell survival under hypoxic
462 conditions in colorectal cancer and glioma, respectively (42,44). However, N-acetyl
463 cysteine, a potent antioxidant, failed to rescue viability of PCa cells upon MTHFD2
464 knockdown suggesting that altered redox homeostasis may not be the primary reason
465 for MTHFD2 knockdown-mediated cell death (**Supp. Figure 9**).

466 MTHFD2 also participates in the formation of formylmethionyl transfer RNA (fMet)
467 that is required for the initiation of protein synthesis in the mitochondria, thereby
468 regulating mitochondrial protein translation (**Figure 1B**), suggesting that its inhibition
469 may impair mitochondria genesis and/or biology. However, in preliminary experiments
470 we did not observe any decrease in the number of mitochondria or mitochondrial
471 membrane potential upon MTHFD2 knockdown (**Supp. Figures 10A-C**);
472 nevertheless, it is still possible that the growth advantage that is contributed by
473 MTHFD2 to PCa cells is due to its effects on mitochondrial homeostasis.

474 Previous research has shown that the key regulator of protein synthesis mTORC1
475 can activate ATF4 through mechanisms distinct from its canonical induction by stress
476 cascades (22,45). However, according to a recent study, only a very small subset (61
477 genes) of ATF4 regulated genes are actually induced by both mTOR/ATF4 and
478 PERK/ATF4 cascades (46). All three mitochondrial 1C cycle enzymes (MTHFD2,
479 SHMT2, and MTHFD1L) were among these genes, but not the two cytosolic
480 counterparts (MTHFD1 and SHMT1). This study was performed on normal mouse
481 embryonic fibroblasts suggesting that ATF4-mediated metabolic regulation is not
482 specific to cancer cells.

483 Furthermore, our analysis on the GTEx and TCGA datasets suggested that in PCa
484 tumors cascades other than mTORC1/ATF4 signaling are also involved in regulation
485 of the m1C cycle (**Figure 6A**). In particular, c-MYC-associated gene expression was
486 highly correlated with m1C gene expression in PCa. Together with the other data we
487 present here, this suggested that ATF4 and c-MYC may coordinately regulate m1C
488 gene expression. Consistent with this, the ATF4 binding sites in the vicinity of m1C
489 enzymes from our ChIP-Seq analysis coincide with those of c-MYC that were
490 identified earlier (**Figure 7A**) (30). Furthermore, both mRNA and protein levels of
491 MTHFD2 were inhibited upon c-MYC knockdown. These observations are intriguing
492 as c-MYC is an established oncoprotein for PCa, and we have recently identified it as
493 a downstream target and mediator of the IRE1-XBP1s arm of the unfolded protein
494 response (UPR) (10,47). Our data thus establish a new role of c-MYC in modulating

495 the UPR and a potential novel mode of crosstalk between the IRE1-XBP1s and
496 PERK-eIF2 α -ATF4 signaling.

497 Based on our findings herein and recently published studies, we suggest the
498 following model (Figure7F): Under normal conditions, ATF4 regulates m1C gene
499 expression, whereas c-MYC is involved in regulating both m1C and c1C gene
500 expression. Under conditions of some types of stress, c-MYC expression is
501 downregulated, and ATF4 can compensate for this to sustain the expression of the
502 m1C cycle gene expression, whereas c1C gene expression remains low. However,
503 in tumors, various mechanisms, such as c-MYC gene amplification and activation of
504 the IRE1/XBP1 cascade, can keep c-MYC expression high resulting in further
505 elevated levels of m1C gene expression, which will satisfy the metabolic needs of the
506 cancer cell in cooperation with UPR-mediated ATF4 signaling. These data thus
507 establish that UPR activation can induce m1C cycle by promoting both ATF4 and c-
508 MYC expression. There may be other points of interaction of c-MYC with the UPR in
509 PCa to establish autoregulatory mechanisms, such as c-MYC heterodimerization with
510 XBP1s to activate the IRE1-XBP1s pathway, which then activates c-MYC expression,
511 as observed in breast cancer cells (48,49) (for a review, see (50)). Thus there
512 appears to be feedback loops that are likely to be responsive to environmental cues
513 and determine the outcome of the interactions between ATF4 and c-MYC signaling,
514 which converge on activation of m1C expression.

515

516 In summary, our findings establish an interplay between ATF4 and c-MYC to drive
517 m1C cycle gene expression as a critical component for PCa growth. As exemplified
518 by the dramatic tumor inhibitory effects of MTHFD2 targeting *in vivo* and the robust
519 prognostic value of the m1C gene signature, future work should further evaluate the
520 m1C cycle as a potential biomarker and/or therapeutic target in PCa.

521

522 **Acknowledgments**

523 We thank all members of the FS laboratory for helpful discussions. This work was
524 supported by grants from the Norwegian Research Council (#193337), Norwegian

525 Cancer Society (#419204), and Health South East Norway (#36024) to FS.

526 References

- 527 1. Locasale JW, Cantley LC. Metabolic flux and the regulation of mammalian cell
528 growth. *Cell metabolism* **2011**;14:443-51
- 529 2. Locasale JW. Serine, glycine and one-carbon units: cancer metabolism in full
530 circle. *Nat Rev Cancer* **2013**;13:572-83
- 531 3. Meiser J, Vazquez A. Give it or take it: the flux of one-carbon in cancer cells.
532 *FEBS J* **2016**;283:3695-704
- 533 4. Nilsson R, Jain M, Madhusudhan N, Sheppard NG, Strittmatter L, Kampf C, *et*
534 *al.* Metabolic enzyme expression highlights a key role for MTHFD2 and the
535 mitochondrial folate pathway in cancer. *Nat Commun* **2014**;5:3128
- 536 5. Di Pietro E, Sirois J, Tremblay ML, MacKenzie RE. Mitochondrial NAD-
537 dependent methylenetetrahydrofolate dehydrogenase-
538 methenyltetrahydrofolate cyclohydrolase is essential for embryonic
539 development. *Molecular and cellular biology* **2002**;22:4158-66
- 540 6. Vazquez A, Tedeschi PM, Bertino JR. Overexpression of the mitochondrial
541 folate and glycine-serine pathway: a new determinant of methotrexate
542 selectivity in tumors. *Cancer Res* **2013**;73:478-82
- 543 7. Siegel RL, Miller KD, Jemal A. Cancer statistics, 2020. *CA Cancer J Clin*
544 **2020**;70:7-30
- 545 8. Sheng X, Arnoldussen YJ, Storm M, Tesikova M, Nenseth HZ, Zhao S, *et al.*
546 Divergent androgen regulation of unfolded protein response pathways drives
547 prostate cancer. *EMBO Mol Med* **2015**;7:788-801
- 548 9. Pallmann N, Livgard M, Tesikova M, Zeynep Nenseth H, Akkus E, Sikkeland J,
549 *et al.* Regulation of the unfolded protein response through ATF4 and FAM129A
550 in prostate cancer. *Oncogene* **2019**;38:6301-18
- 551 10. Sheng X, Nenseth HZ, Qu S, Kuzu OF, Frahnaw T, Simon L, *et al.* IRE1alpha-
552 XBP1s pathway promotes prostate cancer by activating c-MYC signaling. *Nat*
553 *Commun* **2019**;10:323
- 554 11. Ducker GS, Rabinowitz JD. One-Carbon Metabolism in Health and Disease.
555 *Cell metabolism* **2017**;25:27-42
- 556 12. Luhr M, Torgersen ML, Szalai P, Hashim A, Brech A, Staerk J, *et al.* The
557 kinase PERK and the transcription factor ATF4 play distinct and essential roles
558 in autophagy resulting from tunicamycin-induced ER stress. *J Biol Chem*
559 **2019**;294:8197-217
- 560 13. Tibbetts AS, Appling DR. Compartmentalization of Mammalian folate-mediated
561 one-carbon metabolism. *Annu Rev Nutr* **2010**;30:57-81
- 562 14. Nguyen HM, Vessella RL, Morrissey C, Brown LG, Coleman IM, Higano CS, *et*
563 *al.* LuCaP Prostate Cancer Patient-Derived Xenografts Reflect the Molecular
564 Heterogeneity of Advanced Disease and Serve as Models for Evaluating
565 Cancer Therapeutics. *Prostate* **2017**;77:654-71

- 566 15. Jin Y, Wang L, Qu S, Sheng X, Kristian A, Maelandsmo GM, *et al.* STAMP2
567 increases oxidative stress and is critical for prostate cancer. *EMBO Mol Med*
568 **2015**;7:315-31
- 569 16. Jin Y, Qu S, Tesikova M, Wang L, Kristian A, Maelandsmo GM, *et al.*
570 Molecular circuit involving KLK4 integrates androgen and mTOR signaling in
571 prostate cancer. *Proceedings of the National Academy of Sciences of the*
572 *United States of America* **2013**;110:E2572-81
- 573 17. Taylor BS, Schultz N, Hieronymus H, Gopalan A, Xiao Y, Carver BS, *et al.*
574 Integrative genomic profiling of human prostate cancer. *Cancer cell*
575 **2010**;18:11-22
- 576 18. Vanaja DK, Chevillet JC, Iturria SJ, Young CY. Transcriptional silencing of zinc
577 finger protein 185 identified by expression profiling is associated with prostate
578 cancer progression. *Cancer Res* **2003**;63:3877-82
- 579 19. Lapointe J, Li C, Higgins JP, van de Rijn M, Bair E, Montgomery K, *et al.* Gene
580 expression profiling identifies clinically relevant subtypes of prostate cancer.
581 *Proceedings of the National Academy of Sciences of the United States of*
582 *America* **2004**;101:811-6
- 583 20. LaTulippe E, Satagopan J, Smith A, Scher H, Scardino P, Reuter V, *et al.*
584 Comprehensive gene expression analysis of prostate cancer reveals distinct
585 transcriptional programs associated with metastatic disease. *Cancer Res*
586 **2002**;62:4499-506
- 587 21. Singh D, Febbo PG, Ross K, Jackson DG, Manola J, Ladd C, *et al.* Gene
588 expression correlates of clinical prostate cancer behavior. *Cancer cell*
589 **2002**;1:203-9
- 590 22. Park Y, Reyna-Neyra A, Philippe L, Thoreen CC. mTORC1 Balances Cellular
591 Amino Acid Supply with Demand for Protein Synthesis through Post-
592 transcriptional Control of ATF4. *Cell Rep* **2017**;19:1083-90
- 593 23. Harding HP, Zhang Y, Zeng H, Novoa I, Lu PD, Calton M, *et al.* An integrated
594 stress response regulates amino acid metabolism and resistance to oxidative
595 stress. *Molecular cell* **2003**;11:619-33
- 596 24. Xing C, Ci X, Sun X, Fu X, Zhang Z, Dong EN, *et al.* Klf5 deletion promotes
597 Pten deletion-initiated luminal-type mouse prostate tumors through multiple
598 oncogenic signaling pathways. *Neoplasia* **2014**;16:883-99
- 599 25. Cowling VH, D'Cruz CM, Chodosh LA, Cole MD. c-Myc transforms human
600 mammary epithelial cells through repression of the Wnt inhibitors DKK1 and
601 SFRP1. *Molecular and cellular biology* **2007**;27:5135-46
- 602 26. Zheng L, Sun D, Fan W, Zhang Z, Li Q, Jiang T. Diagnostic value of SFRP1 as
603 a favorable predictive and prognostic biomarker in patients with prostate
604 cancer. *PloS one* **2015**;10:e0118276
- 605 27. Anderson PD, McKissic SA, Logan M, Roh M, Franco OE, Wang J, *et al.*
606 Nkx3.1 and Myc crossregulate shared target genes in mouse and human
607 prostate tumorigenesis. *J Clin Invest* **2012**;122:1907-19
- 608 28. Nusinow DP, Szpyt J, Ghandi M, Rose CM, McDonald ER, 3rd, Kalocsay M, *et*
609 *al.* Quantitative Proteomics of the Cancer Cell Line Encyclopedia. *Cell*
610 **2020**;180:387-402 e16

- 611 29. Tameire F, Verginadis, II, Leli NM, Polte C, Conn CS, Ojha R, *et al.* ATF4
612 couples MYC-dependent translational activity to bioenergetic demands during
613 tumour progression. *Nature cell biology* **2019**;21:889-99
- 614 30. Barfeld SJ, Urbanucci A, Itkonen HM, Fazli L, Hicks JL, Thiede B, *et al.* c-Myc
615 Antagonises the Transcriptional Activity of the Androgen Receptor in Prostate
616 Cancer Affecting Key Gene Networks. *EBioMedicine* **2017**;18:83-93
- 617 31. Faubert B, Solmonson A, DeBerardinis RJ. Metabolic reprogramming and
618 cancer progression. *Science* **2020**;368
- 619 32. Yoshida GJ. Metabolic reprogramming: the emerging concept and associated
620 therapeutic strategies. *Journal of experimental & clinical cancer research : CR*
621 **2015**;34:111
- 622 33. Sun H, Zhou Y, Skaro MF, Wu Y, Qu Z, Mao F, *et al.* Metabolic
623 Reprogramming in Cancer Is Induced to Increase Proton Production. *Cancer*
624 *Res* **2020**;80:1143-55
- 625 34. Wang Y, Ning Y, Alam GN, Jankowski BM, Dong Z, Nor JE, *et al.* Amino acid
626 deprivation promotes tumor angiogenesis through the GCN2/ATF4 pathway.
627 *Neoplasia* **2013**;15:989-97
- 628 35. DeNicola GM, Chen PH, Mullarky E, Sudderth JA, Hu Z, Wu D, *et al.* NRF2
629 regulates serine biosynthesis in non-small cell lung cancer. *Nature genetics*
630 **2015**;47:1475-81
- 631 36. Possemato R, Marks KM, Shaul YD, Pacold ME, Kim D, Birsoy K, *et al.*
632 Functional genomics reveal that the serine synthesis pathway is essential in
633 breast cancer. *Nature* **2011**;476:346-50
- 634 37. Sun L, Song L, Wan Q, Wu G, Li X, Wang Y, *et al.* cMyc-mediated activation of
635 serine biosynthesis pathway is critical for cancer progression under nutrient
636 deprivation conditions. *Cell research* **2015**;25:429-44
- 637 38. Vie N, Copois V, Bascoul-Mollevi C, Denis V, Bec N, Robert B, *et al.*
638 Overexpression of phosphoserine aminotransferase PSAT1 stimulates cell
639 growth and increases chemoresistance of colon cancer cells. *Molecular cancer*
640 **2008**;7:14
- 641 39. Lane AN, Fan TW. Regulation of mammalian nucleotide metabolism and
642 biosynthesis. *Nucleic Acids Res* **2015**;43:2466-85
- 643 40. Ducker GS, Chen L, Morscher RJ, Ghergurovich JM, Esposito M, Teng X, *et*
644 *al.* Reversal of Cytosolic One-Carbon Flux Compensates for Loss of the
645 Mitochondrial Folate Pathway. *Cell metabolism* **2016**;23:1140-53
- 646 41. Shin M, Momb J, Appling DR. Human mitochondrial MTHFD2 is a dual redox
647 cofactor-specific methylenetetrahydrofolate
648 dehydrogenase/methenyltetrahydrofolate cyclohydrolase. *Cancer Metab*
649 **2017**;5:11
- 650 42. Ye J, Fan J, Venneti S, Wan YW, Pawel BR, Zhang J, *et al.* Serine catabolism
651 regulates mitochondrial redox control during hypoxia. *Cancer Discov*
652 **2014**;4:1406-17
- 653 43. Martinez-Reyes I, Chandel NS. Mitochondrial one-carbon metabolism
654 maintains redox balance during hypoxia. *Cancer Discov* **2014**;4:1371-3
- 655 44. Ju HQ, Lu YX, Chen DL, Zuo ZX, Liu ZX, Wu QN, *et al.* Modulation of Redox
656 Homeostasis by Inhibition of MTHFD2 in Colorectal Cancer: Mechanisms and

657 Therapeutic Implications. Journal of the National Cancer Institute
658 **2019**;111:584-96

659 45. Ben-Sahra I, Hoxhaj G, Ricoult SJH, Asara JM, Manning BD. mTORC1
660 induces purine synthesis through control of the mitochondrial tetrahydrofolate
661 cycle. Science **2016**;351:728-33

662 46. Torrence ME, MacArthur MR, Hosios AM, Valvezan AJ, Asara JM, Mitchell JR,
663 *et al.* The mTORC1-mediated activation of ATF4 promotes protein and
664 glutathione synthesis downstream of growth signals. Elife **2021**;10

665 47. Koh CM, Bieberich CJ, Dang CV, Nelson WG, Yegnasubramanian S, De
666 Marzo AM. MYC and Prostate Cancer. Genes Cancer **2010**;1:617-28

667 48. Zhao N, Cao J, Xu L, Tang Q, Dobrolecki LE, Lv X, *et al.* Pharmacological
668 targeting of MYC-regulated IRE1/XBP1 pathway suppresses MYC-driven
669 breast cancer. J Clin Invest **2018**;128:1283-99

670 49. Sheng X, Nenseth HZ, Qu S, Kuzu O, Frahnaw T, Simon L, *et al.* IRE1 α -
671 XBP1s pathway promotes prostate cancer by activating c-MYC signaling.
672 Nature Communications **2019**;10:323-34

673 50. Jin Y, Saatcioglu F. Targeting the Unfolded Protein Response in Hormone-
674 Regulated Cancers. Trends Cancer **2020**;6:160-71
675

676 **Figure Legends**

677 **Figure 1: ATF4 binds to and regulates expression of mitochondrial but not**
678 **cytoplasmic 1C metabolism genes.** **A.** Venn diagram depicting the number of
679 genes affected by the different analyses (microarray gene expression in yellow, mass
680 spectrometry (MS) in blue, and ChIP-Seq in light red) and their intersections, upon
681 ATF4 knockdown. **B.** A simplified diagram showing c1C and m1C metabolic
682 pathways. **C.** ChIP-Seq analyses of ATF4 target genes reveal strong binding sites in
683 the vicinity of genes that encode m1C cycle enzymes. The GTRD (Gene
684 Transcription Regulation Database) lane shows the number of ATF4 peak calls and
685 their location based on this database. Conservation track shows conservation among
686 vertebrate genomes (phastCons scores). **D.** Summary of 1C metabolism gene
687 regulation in cancer versus normal tissues in the Oncomine database (Top 5%
688 threshold). Darker color in each box indicates larger number of studies and thus
689 more significant association. **E.** Diagram showing the correlation of cancer cell line
690 dependency profiles between m1C metabolism genes and their functionally relevant
691 neighbors. In contrast to the others, ATF4-regulated m1C cycle genes are more
692 strongly linked to each other (red lines). m1C and c1C cycle genes are represented
693 by blue and red boxes, respectively. The numbers in the ovals on the connectors
694 show Pearson correlation coefficients between the linked genes. The red lines have
695 a Pearson correlation coefficient that is greater than 0.15.

696

697 **Figure 2: ATF4 induces expression of mitochondrial but not cytoplasmic 1C**
698 **cycle enzymes.** **A.** siRNA-mediated ATF4 knockdown decreases expression of
699 serine synthesis and m1C cycle enzyme gene expression, but not that of c1C cycle.
700 LNCaP cells were transfected with either control or two independent ATF4-specific
701 siRNAs, treated with Tg (300 nM for 5 h), and were analyzed by qPCR. The
702 efficiency of ATF4 knockdown was confirmed by western analysis as shown in the
703 inset. **B.** Expression of genes encoding serine synthesis and 1C cycle enzymes were
704 analyzed by qPCR upon treatment of LNCaP cells with Tg (30 nM) for the indicated
705 time points. Inset shows ATF4 protein levels upon Tg treatment in the time course
706 experiment. **C.** Data extracted from a RNA-sequencing experiment that was

707 published previously (12). LNCaP cells were transfected with non-targeting siRNA
708 (siCTRL) or two distinct ATF4-targeting siRNAs. Cells were then either treated with
709 DMSO as control or tunicamycin (2.5 μ g/mL for 18 hrs). RNA was isolated and
710 subjected to RNA-sequencing. **D.** ATF4 knockdown decreases MTHFD2 protein
711 expression in multiple PCa cell lines. Indicated cell lines were transfected with either
712 control siRNA or two independent siRNAs targeting ATF4. Cells were treated with Tg
713 (30 nM, 5hr), harvested, and used in Western analysis. **E.** Downregulation of m1C
714 gene expression upon ATF4 knockdown is rescued by ATF4 re-expression.
715 Doxycycline inducible LNCaP-ATF4 cells were transfected either with scrambled
716 siRNA or an ATF4-specific siRNA targeting the 5'-UTR of the gene (siATF4); 4 days
717 later cells were treated with Tg (30 nM for 5h). Doxycycline-mediated induction of
718 ATF4 effectively restored MTHFD2 levels as analyzed by qPCR. **F.** Under non-
719 stressed conditions, despite its high mRNA expression, ATF4 is not translated to a
720 significant protein level, hence its knockdown fails to down-regulate MTHFD2 levels.
721 Doxycycline-inducible LNCaP-ATF4 cells were transfected either with scrambled
722 siRNA or two independent siRNAs targeting the open reading frame (siATF4 #1) or
723 5'-UTR (siATF4 #2) of the ATF4 mRNA. At the same time with the transfection, cells
724 were treated with indicated amounts of doxycycline to induce ATF4 expression and
725 processed after 48 hrs. Note that ectopic ATF4 expression (upon Dox treatment)
726 effectively upregulates MTHFD2 levels while downregulating endogenous ATF4
727 levels (detected by UTR specific primers). ASNS expression, a well-characterized
728 ATF4 target gene, is shown as a reporter of ATF4 activity. #: $p < 0.001$; ^: $p < 0.01$; *:
729 0.05; ns: non-significant. **G.** Individual CHIP analysis verified ATF4 binding to the
730 intronic region (chr2:74,426,212-74,426,487 – hg19) of the MTHFD2 gene identified
731 in the CHIP-Seq experiment. LNCaP cells were transfected with either scrambled
732 siRNA or ATF4-specific siRNA, treated with vehicle or Tg, and CHIP assay was
733 performed using an ATF4-specific antibody.

734 **Figure 3: MTHFD2 knockdown inhibits growth of PCa cells, PDX-derived**
735 **organoids, and tumor xenografts.** **A.** MTHFD2 knockdown efficiency was
736 determined in LNCaP and DU145 cells that were transfected with either scrambled

737 siRNA or two independent MTHFD2-specific siRNAs for 48 hours by both qPCR and
738 Western analyses. **B.** LNCaP, VCaP, or 22Rv1 cells transfected with control or
739 MTHFD2-specific siRNAs were cultured for the indicated times, and cell numbers
740 were determined by trypan blue staining. * $p < 0.01$. MTHFD2 knockdown hinders
741 colony (**C-D**) and prostatosphere (**E**) formation ability of PCa cells. Indicated cells
742 were transfected with control siRNA or MTHFD2-specific siRNAs and cultured for two
743 weeks. Colonies formed were stained and quantified as described in Materials and
744 Methods. Prostatospheres were pictured and counted under a light microscope;
745 representative areas are presented. **F.** Viability of normal prostate cells is not
746 affected by MTHFD2 knockdown. RWPE1 cells were transfected with either control
747 siRNA or two independent MTHFD2-targeting siRNAs. After 48 hours, relative cell
748 viability and MTHFD2 expression were determined using the CCK8 assay and qPCR,
749 respectively. **G.** MTHFD2 expression and knockdown efficiency in various LuCaP
750 organoids were assessed by Western analysis. **H.** MTHFD2 knockdown significantly
751 decreased LuCaP organoid formation without affecting cell death, in LuCaP 35 and
752 LuCaP 96 that express MTHFD2, but not in LuCaP 136, which does not express
753 MTHFD2. **I.** Nanoliposomal systemic delivery of MTHFD2-specific siRNA profoundly
754 inhibited the growth of VCaP and 22Rv1 xenograft tumors *in vivo*. VCaP and 22Rv1
755 cells were implanted subcutaneously in male nude mice. Once tumors were
756 palpable, mice ($n = 5$ per group) were given either empty nanoliposomes or
757 MTHFD2-specific siRNA as described in Materials and Methods. Tumor volumes
758 were measured at the indicated time points.

759 **Figure 4: MTHFD2 expression is increased in PCa.** **A.** Basal levels of MTHFD2
760 mRNA and protein were determined in various PCa cell lines and the normal prostate
761 cell line by qPCR and Western analysis, respectively. **B.** MTHFD2 expression was
762 analyzed by immunohistochemistry in matched benign prostate and PCa specimens
763 from 24 patients. Representative images and quantification of staining is shown. **C.**
764 Tissue microarrays with normal prostate ($n = 223$) and primary prostate tumors
765 ($n = 860$) were analyzed by immunohistochemistry. Middle panel shows increased
766 MTHFD2 expression with increasing Gleason grade of the samples. Representative
767 images and quantification of staining intensity are shown. **D.** In a subset of the

768 samples used for IHC analysis shown in Figure 5C , the correlation of ATF4 and
769 MTHFD2 staining scores is depicted. r denotes Pearson correlation between the two
770 stainings.

771 **Figure 5: Mitochondrial 1C gene expression is deregulated in PCa and a gene**
772 **expression signature derived from it is strongly associated with PCa**
773 **prognosis. A-B.** Expression of MTHFD2 and SHMT2 is upregulated in primary
774 and/or metastatic PCa compared to benign samples. Expression data were retrieved
775 from the Oncomine database. 1: Singh et al. (21), 2: Taylor et al. (17), 3: Vanaja et al.
776 (18), 4: Lapointe et al. (19), 5: La Tulippe et al. (20), N: Normal, P: Primary, M:
777 Metastatic. **C.** m1C but not c1C cycle genes are upregulated in primary PCa samples
778 in the TCGA dataset. **D.** A gene expression signature consisting of the three ATF4-
779 regulated m1C cycle genes (MTHFD2 + MTHFD1L + SHMT2) is significantly
780 associated with recurrence-free survival in the TCGA dataset. PCa samples were
781 ordered based on the expression of the signature genes and a Kaplan-Meier graph
782 was drawn based on the survival data for top and bottom ~36% of the samples.

783 **Figure 6: Mitochondrial 1C cycle gene expression is differentially regulated in**
784 **benign and PCa tissues. A.** m1C cycle gene expression correlates with ATF4
785 independent target genes of mTORC1 signaling in normal prostate, but not in PCa
786 samples. Pearson correlation coefficients between indicated genes were calculated
787 in the GTEx dataset containing 106 normal prostate tissue samples and TCGA
788 database containing 426 primary PCa samples. Genes in green and red were up and
789 down-regulated, respectively, upon Torin 1 treatment. **B.** Distinct sets of genes
790 correlate with MTHFD2 in normal and PCa samples. Venn diagram shows the
791 number of shared genes that correlate with MTHFD2 in the SEEK, TCGA, or GTEx
792 datasets. In each dataset, the top 500 genes that correlate with MTHFD2 expression
793 were included in the analyses. **C.** ER stress-mediated induction of ATF4 overrides
794 mTORC1/ATF4-mediated MTHFD2 expression. LNCaP cells were treated with 30
795 nM Tg (for 8 hours) and/or 100 nM Rapamycin for 24 hours and expression of m1C
796 cycle genes was determined by qPCR. Bottom panel shows Western analysis
797 verifying the activity of the compounds. **D.** Enrichment analysis of top 500 genes that

798 correlate with MTHFD2 expression in the TCGA dataset. **E.** Prevalence of various
799 mutations among the top and bottom 180 (~36 %) samples in the TCGA dataset
800 based on the expression of the m1C cycle gene signature. **F.** Venn diagram showing
801 proteins that correlate with the three m1C cycle enzyme expression and two
802 mitochondrial DNA encoded proteins (MT-CO1 and MT-ATP8) ($r>0.5$). **G.** Geneset
803 enrichment analysis of 136 proteins that were shared between the MTHFD2 and
804 SHMT2 groups identified in **F.**

805 **Figure 7: c-MYC co-occupies ATF4 response elements and regulates m1C cycle**
806 **gene expression.** **A.** c-MYC ChIP-Seq analyses in LNCaP cells revealed co-
807 localization of ATF4 binding sites that were identified in the proximity of m1C cycle
808 genes and EIF4EBP1. The data were obtained from GSE73994 in which Dox-
809 inducible LNCaP-c-MYC cell line was used. Orange triangles show the location of
810 ATF4 binding sites identified in our ChIP-Seq analysis (Figure 1D). Please note that
811 for all four genes, in contrast to other nearby sites, the c-MYC binding at the ATF4
812 target site was relatively more increased upon c-MYC expression. **B.** CRISPRi-
813 mediated inhibition of *MYC* expression downregulates m1C cycle enzyme genes and
814 *EIF4EBP1* expression in the 22Rv1 PCa cell line. The data were obtained from
815 GSE142808. **C.** Results of a microarray study showing induction of m1C enzyme
816 gene and *EIF4EBP1* expression upon ectopic *c-MYC* expression in LNCaP cells.
817 The data were obtained from GSE73917. **D.** *MYC* knockdown effectively
818 downregulates m1C cycle enzyme genes and *EIF4EBP1* expression. LNCaP cells
819 were transfected with siCTRL or sic-MYC (an siRNA pool), and 48 hrs later
820 processed for qPCR and Western analyses. **E.** Under stress conditions ATF4
821 counterbalances the c-MYC loss to drive m1C gene expression. LNCaP cells were
822 transfected with control, ATF4 and/or c-MYC specific siRNAs, and 48 hrs later treated
823 with DMSO or 30 nM Tg for 5 or 24 hrs. ATF4, MYC and MTHFD2 expressions were
824 determined by qPCR. Under the same conditions, protein levels of c-MYC, ATF4 and
825 MTHFD2 were measured by Western analysis. **F.** Schematic depiction of m1C and
826 c1C cycle gene expression under normal prostate and in PCa. Under normal
827 conditions, ATF4 protein expression is high enough only under transient stress
828 conditions and it specifically induces m1C expression, whereas c-MYC drives both

829 c1C and m1C expression upon transient growth-promoting signals. In tumors, there
830 is chronic stress that activates ATF4 signaling and m1C gene expression. Likewise,
831 various chronic signals, such as proliferative signaling and gene amplification,
832 increase c-MYC expression in PCa tumors that results in higher levels of m1C and
833 c1C gene expression. Having input from both ATF4 and c-MYC, m1C gene
834 expression is markedly higher than that of the c1C cycle in PCa.

Figure 1

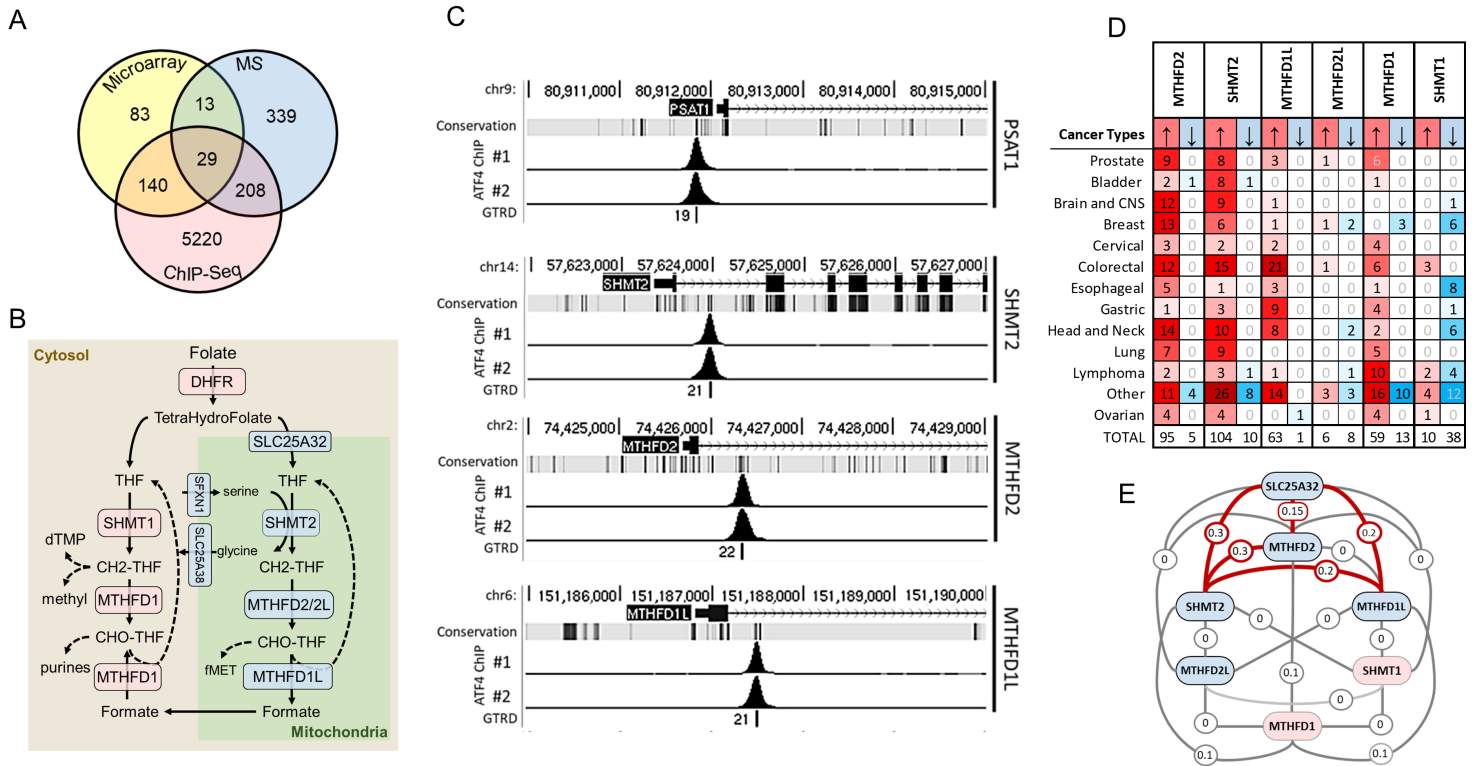


Figure 2

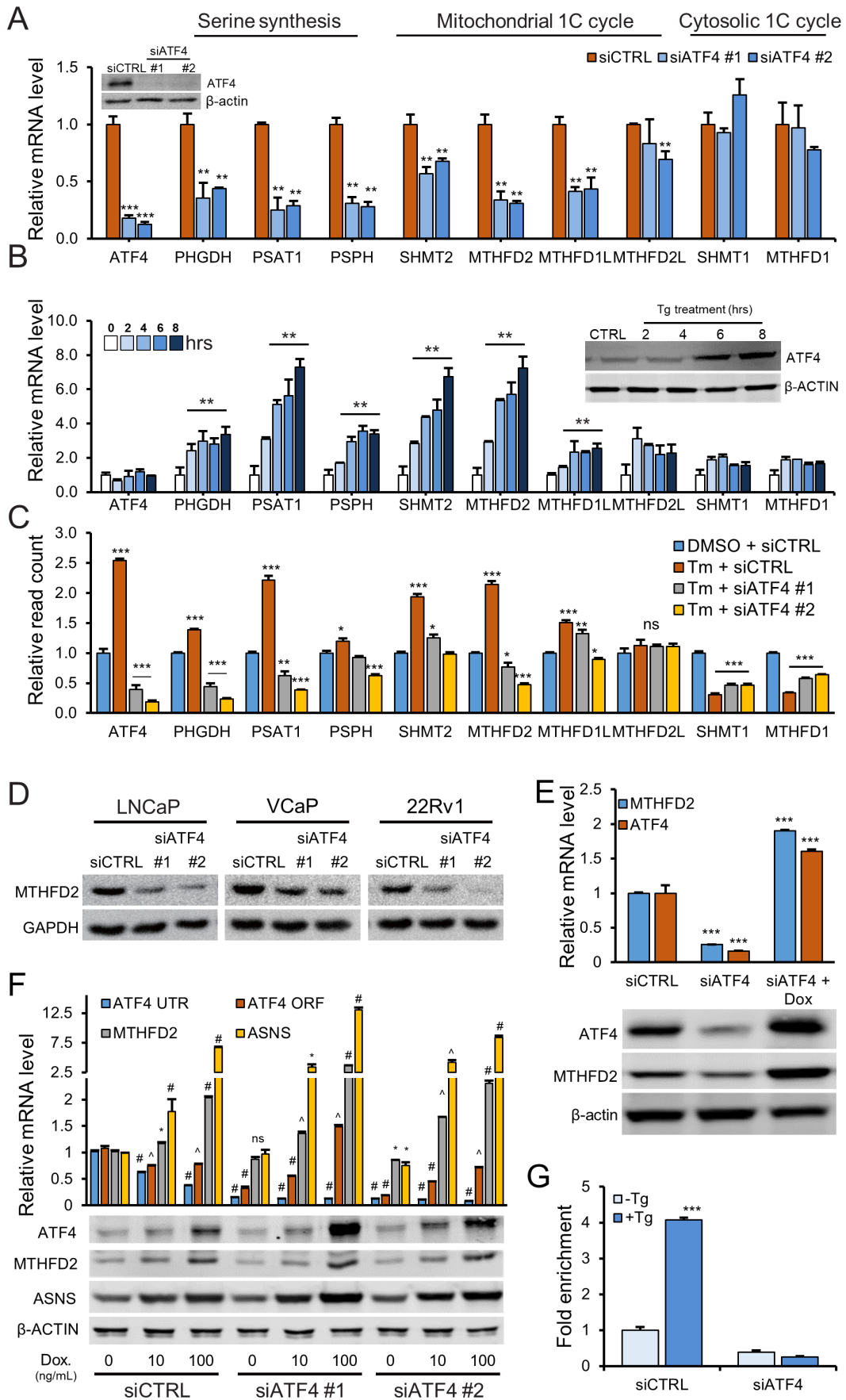


Figure 3

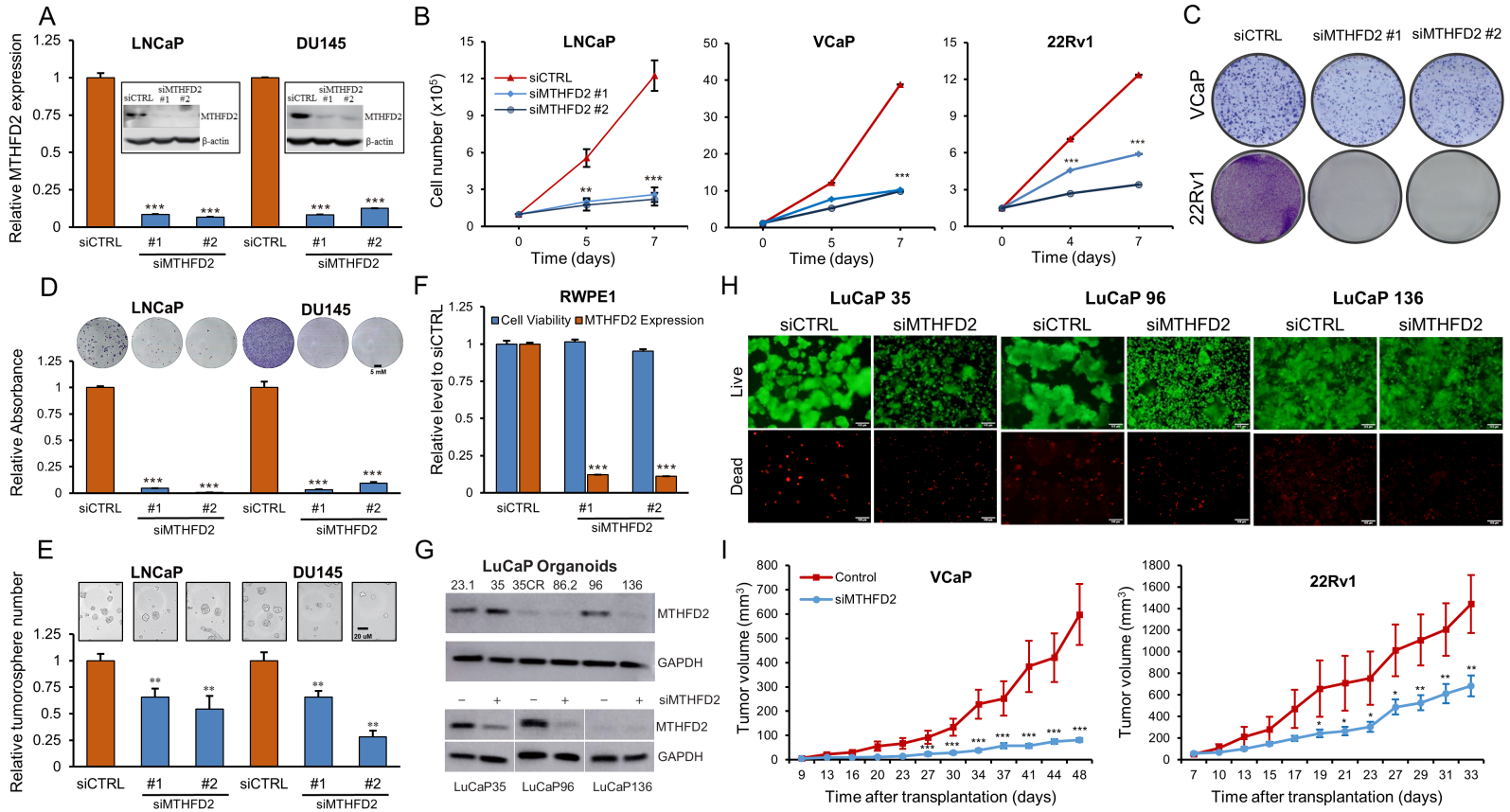


Figure 4

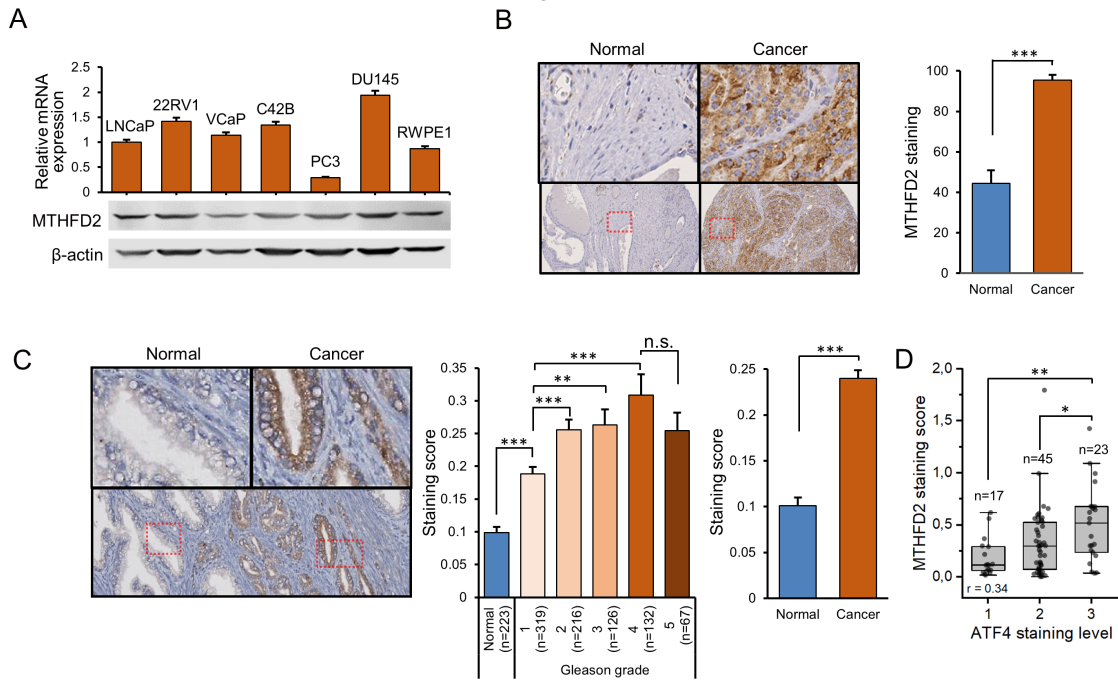
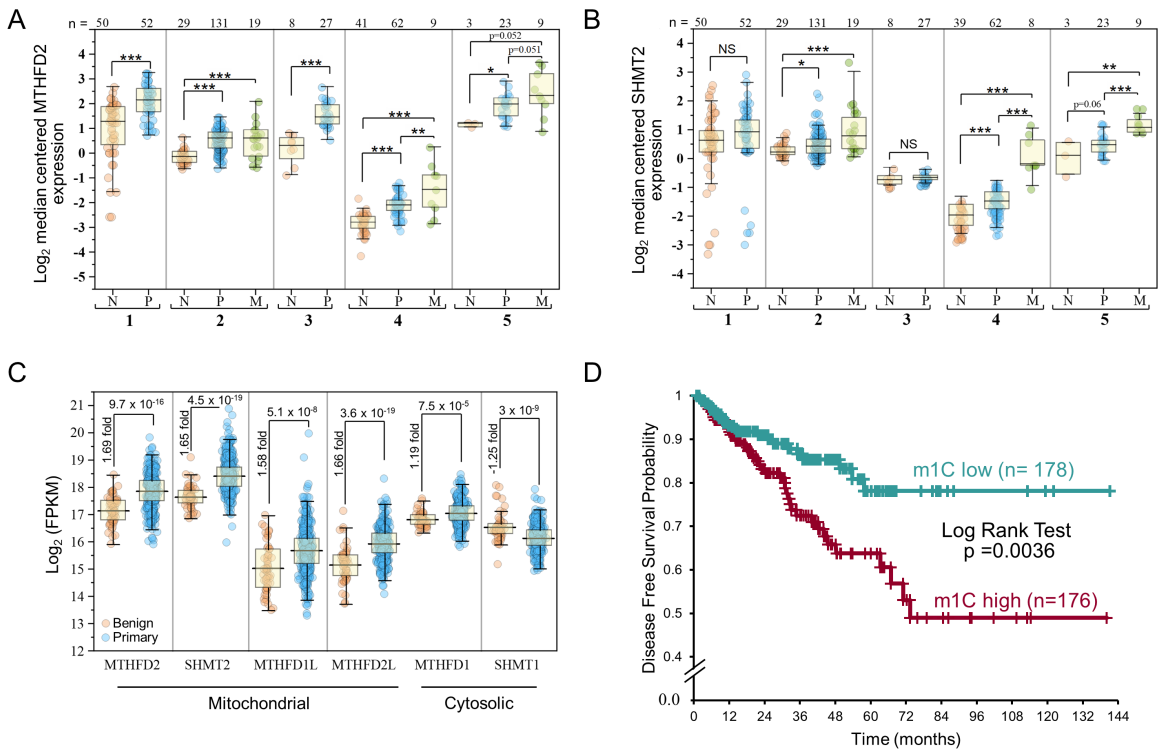


Figure 5



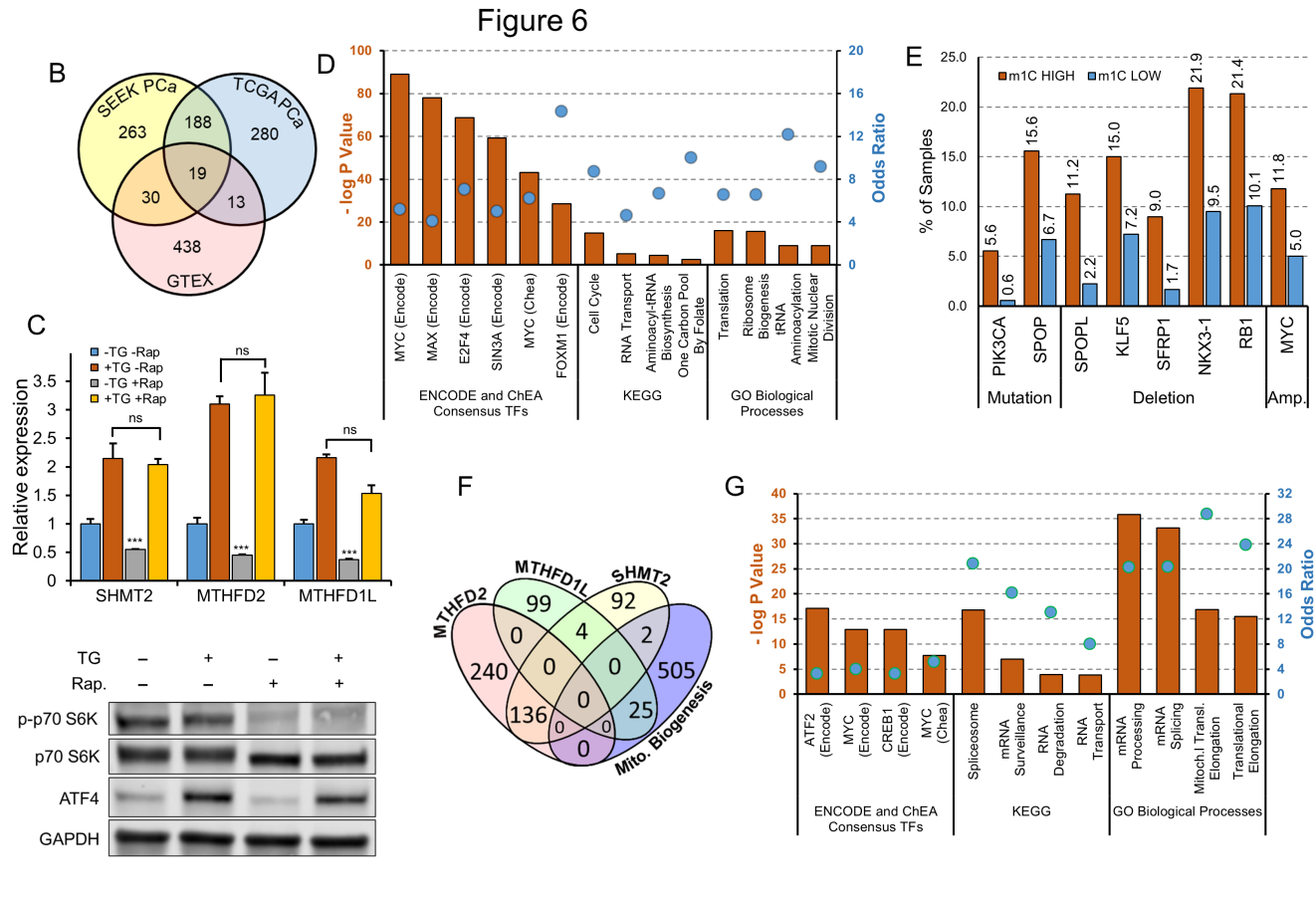
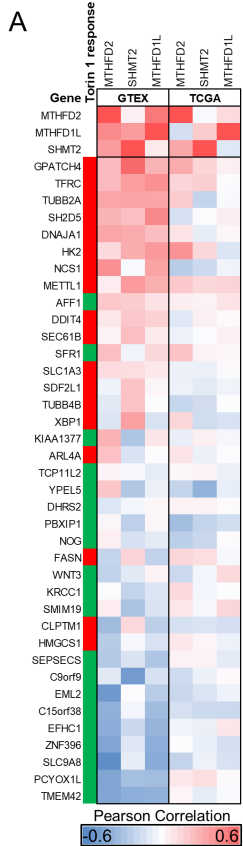


Figure 7

